RC-LACE stay report

Development of the sub-kilometer ALARO Canonical Model Configuration

Mario Hrastinski

In collaboration with: Petra Smoliková

15-26.5.2022. and 9-20.10.2023.

CHMI, Prague, Czech Republic

1 Introduction

During this stay, the development and validation of sub-kilometer ALARO Canonical Model Configuration (CMC) over Central Europe is continued. It is related to the previous two research stays[1, 2] and mainly aims to optimize the settings of horizontal diffusion and upgrade the turbulence scheme by including 3D effects and, ultimately, by making it more scale-aware. The research is also related to the Destine Earth On-Demand Extremes (DEODE) initiative. The report is organized as follows. The methodology used to compute resolved turbulence kinetic energy, i.e., one of the main diagnostic tools, is explained in Section 2. The setup of the utilized numerical model is described in Section 3, followed by the analysis of results in Section 4. Finally, concluding remarks are highlighted in Chapter 5.

2 The computation of resolved turbulence kinetic energy

The partitioning between resolved and subgrid turbulence throughout the resolutions, measured by Turbulence Kinetic Energy (TKE), will be used to estimate the model performance in our research. Following the principles of Reynolds averaging, we assume that turbulent flow (x) can be separated on slowly changing mean fields ($\overline{x}$) and fast varying turbulent perturbations (x'):

$$\mathrm{x} = \overline{\mathrm{x}} + \mathrm{x}' \tag{1}$$

The average is usually taken over some period of time but may also be computed over space or even an ensemble of realizations. During the computation of resolved TKE ($\mathrm{TKE_{res}}$), first, we determine the mean state of three velocity components (u, v and w) by averaging them in time for each grid point of the chosen sub-domain. For that purpose, a simple centered moving average is used:

$$\overline{\mathrm{x}}_{\mathrm{MA}} = \frac{1}{\mathrm{N}} \sum_{\mathrm{i=n-k}}^{\mathrm{n+k}} \mathrm{x_i} \tag{2}$$

where k is the number of values taken before and after the current position in time (n), while N=2k+1 is the length of moving average (N=61; 15 minutes).

Once the mean values are known, perturbations are obtained by subtracting from total values, i.e., the left-hand-side of Eq. (1). Finally, the $\mathrm{TKE_{res}}$, at a given grid spacing (Δx) and position in time (n), is computed as:

$$\mathrm{TKE_{res}} = \frac{1}{2}\left(\mathrm{u}'^2 + \mathrm{v}'^2 + \mathrm{w}'^2\right) \tag{3}$$

Before being shown on plots, the values obtained by Eq. (3) are averaged spatially, i.e., over the sub-domain and then over the time window of 2 hours (between 14^{th} and 16^{th} forecast hour). The latter is chosen to cover the passage of the convective system through the area of interest.

3 Numerical model setup

In this study, we utilize the ALARO-CMC, with a non-hydrostatic dynamical core and ALARO-1vB physics package, on four domains with Δx=4, 2, 1, and 0.5 [km], respectively. All domains roughly cover the same area (Fig. 1a), and related model configurations have the same length of the time step, i.e., Δt=15 [s]. The latter is related to the computation of $\mathrm{TKE_{res}}$ across resolutions, for which it is desirable to have datasets of the same length.

The model is initialized at 00 UTC on 21^{st} June 2018 and driven throughout the 18-hour period on 87 vertical levels of a hybrid mass-based and terrain-following coordinate η. The initial conditions are obtained by interpolating the operational input of the ALARO-CZ model, run at Δx=2.325 km, while lateral boundary conditions are obtained from the global model ARPEGE (with 3-hour coupling frequency). The aim is to capture and analyze the convective system passing in the west-east direction through the area denoted with a blue rectangle in Fig. 1b.

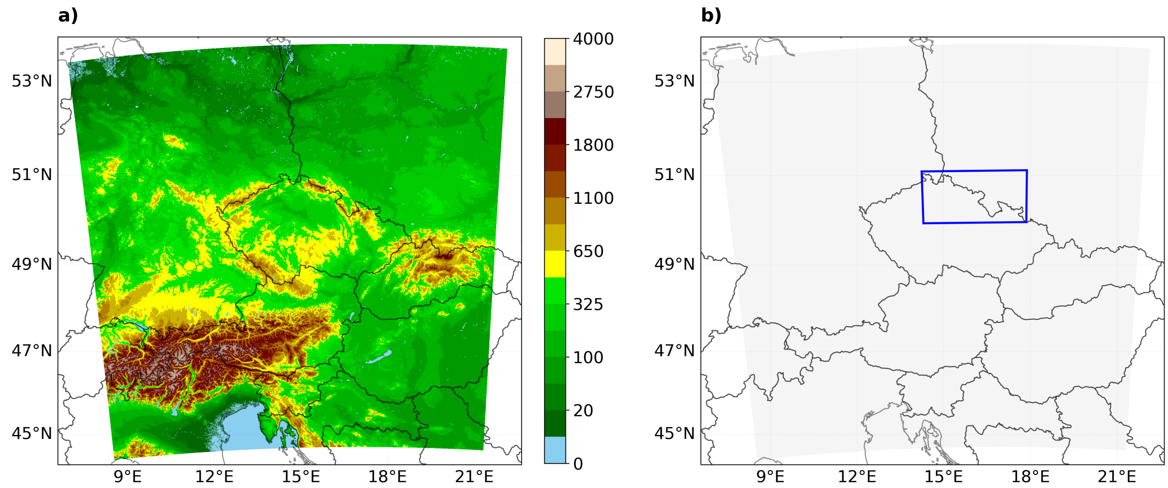

Figure 1: a) Orography of the model domain at $\Delta x = 1$ km and **b)** sub-domain for computation of resolved Turbulence Kinetic Energy (TKE_{res}; blue rectangle).

4 The results of numerical simulations

During the analysis of results, we utilize the following diagnostic tools: chosen 3D prognostic fields (in particular wind components and pressure departure), Kinetic Energy Spectra (KES) obtained with ECTO and averaged profiles of resolved (TKE_{res}), subgrid (TKE_{sbg}) and total TKE (TKE_{tot}). The latter are computed over a sub-domain denoted with a blue rectangle in Fig. 1b. The impact of horizontal resolution and different model settings at the sub-kilometer domain are shown in the following subsections.

4.1 The impact of the horizontal resolution

As expected, the amount of TKE_{res} increases with horizontal resolution (Fig. 2a) while TKE_{sbg} decreases (Fig. 2b). Their sum (TKE_{tot}) is nearly conserved for the two coarsest model configurations (Fig. 2c). However, the remaining two do not follow such a behaviour, and the departure from the target value increases with the horizontal resolution (Fig. 2c). The share of TKE_{res} in TKE_{tot}, for all four configurations, is shown on Fig. 2d and its behavior is generally expected.

The comparison of TKE_{res} profiles indicates that resolved turbulence is overestimated at the sub-kilometer grid. In particular between the Planetary Boundary Layer (PBL) top ($\sim$ level

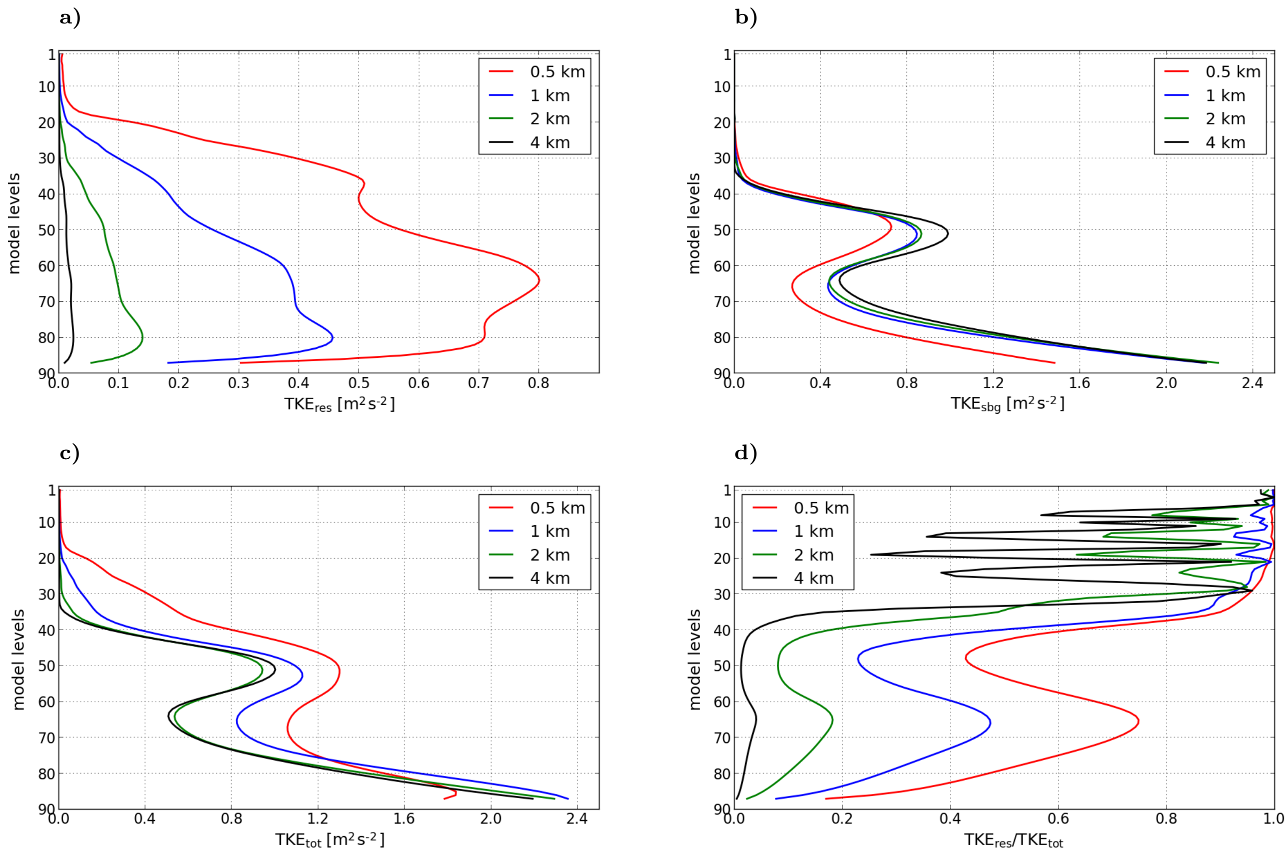

Figure 2: Spatially (over sub-domain on Fig. 1b) and temporally (between 14th and 16th hour) averaged: **a)** resolved Turbulence Kinetic Energy (TKE), **b)** subgrid TKE, **c)** total TKE and **d)** share of resolved TKE across different horizontal resolutions for the forecast initialized at 00 UTC 21st June 2018.

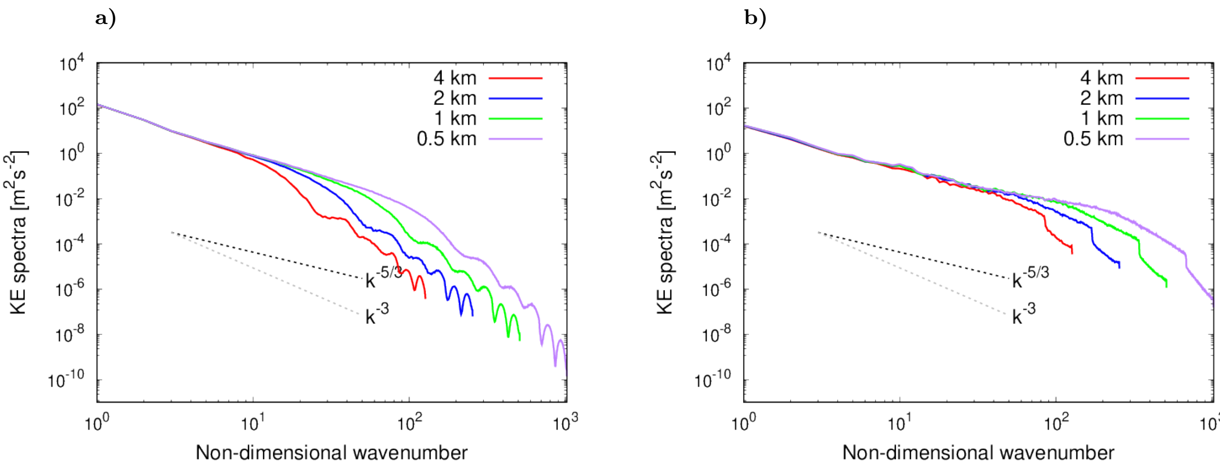

Figure 3: Kinetic energy spectra (KES) at 15 UTC 21st June 2018 across different horizontal resolutions on: **a)** level 20 and **b)** level 80.

60) and tropopause ($\sim$ level 20). On the other hand, the amount of TKE_{sbg} seems to be underestimated in the lower troposphere, i.e., below level 50. The analysis of KES indicates that with an increase in the horizontal resolution, more energy is accumulated near the tail of the spectrum and closer to the surface (Fig. 3a-b). Finally, the analysis of pressure departure fields shows that the amount of small-scale noise increases with resolution (Fig. 4a-d). Although the latter is shown on a single level, behaviour is generally the same throughout the profile.

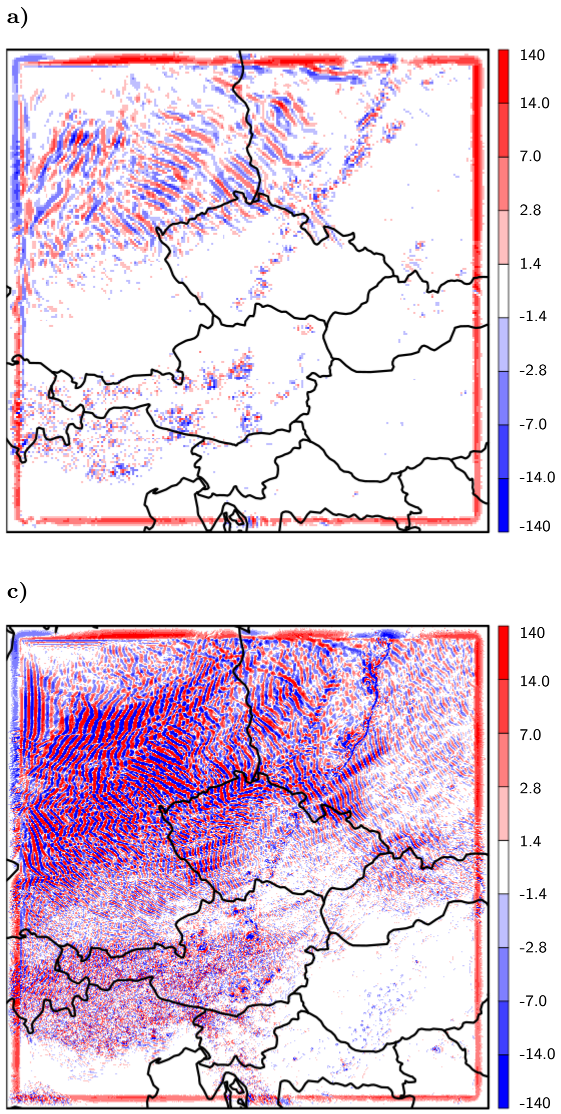

Figure 4: Pressure departure field at 15 UTC 21st June 2018 on model level 60 for: **a)** $\Delta x = 4$ km, **b)** $\Delta x = 2$ km, **c)** $\Delta x = 1$ km and **d)** $\Delta x = 0.5$ km.

Based on the above results, it is clear that settings of the horizontal diffusion, i.e., its three components used in ALARO-CMC, need to be optimized. Further, for consistency reasons, we have utilized deep convection (3MT) and gravity wave drag (GWD) schemes in all four configurations. The impact of both needs to be addressed. Finally, there is possibility that the subgrid turbulence scheme is not adequately adapting at (sub)-kilometer grid. All the above will be the subject of analyses that follow.

4.2 The impact of resolved physical processes and alternative for horizontal diffusion

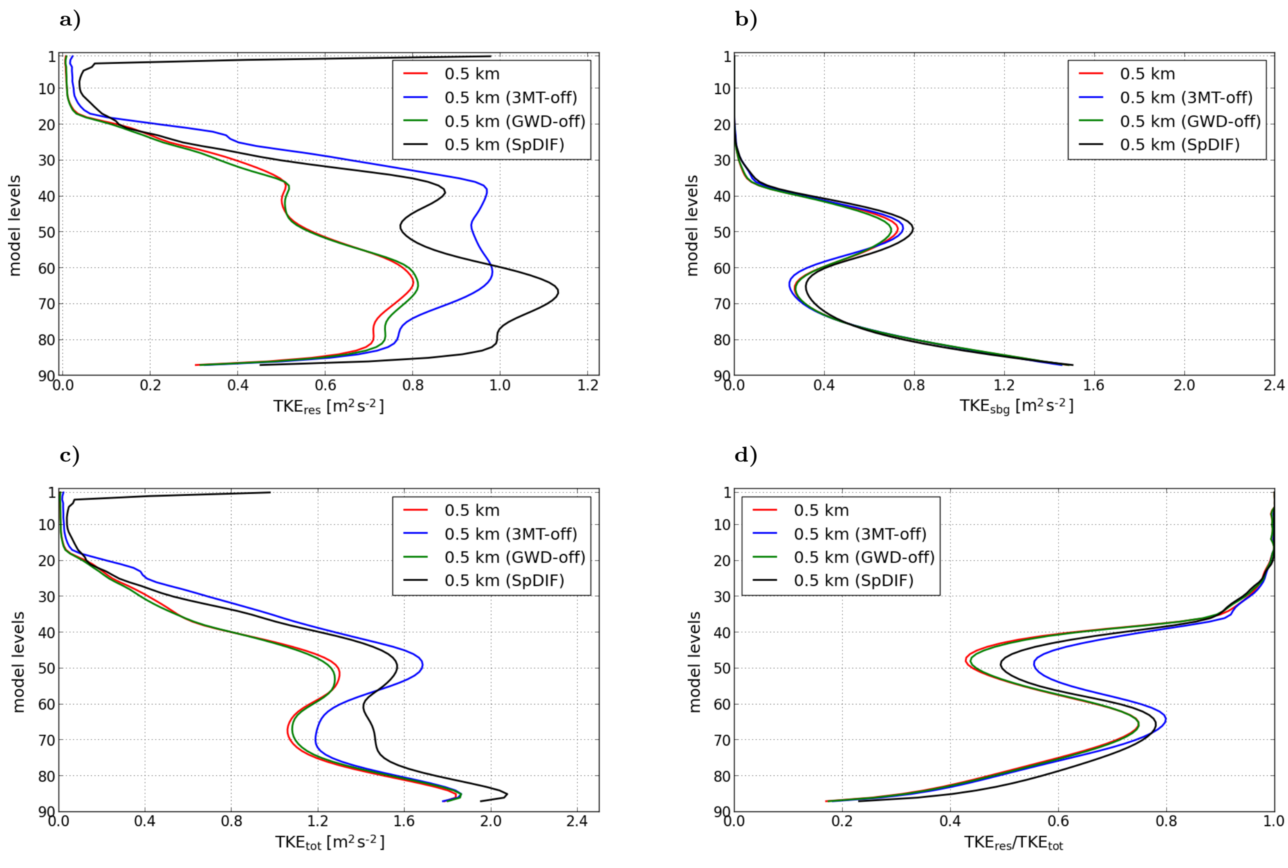

Figure 5: Spatially (over sub-domain on Fig. 1b) and temporally (between 14th and 16th hour) averaged: **a)** resolved Turbulence Kinetic Energy (TKE), **b)** subgrid TKE, **c)** total TKE and **d)** share of resolved TKE at Δx=500 [m] for the forecast initialized at 00 UTC 21st June 2018. The reference (red) is the same as on Fig. 2, 3MT-off and GWD-off have either deep convection (blue) or gravity wave drag scheme (green) switched off, while in SpDIF (black), three-component horizontal diffusion (used by default in ALARO-CMC) is replaced with full spectral diffusion of the operational AROME-MF.

Since the challenges at $\Delta x = 0.5$ km seem to be larger, and this is also the working resolution in the scope of DEODE initiative, further experiments aim at identifying sources of related problems and attempts to correct them. First, we test the impact of 3MT and GWD schemes, i.e., deep convection and gravity wave drag processes, which should be resolved at this resolution. The profiles of $\mathrm{TKE_{tot}}$ and its components, i.e., $\mathrm{TKE_{res}}$ and $\mathrm{TKE_{sbg}}$, are shown on Fig. 5a-c. The impact of GWD scheme on $\mathrm{TKE_{res}}$ is small. On the other hand, the impact of 3MT on $\mathrm{TKE_{res}}$ and $\mathrm{TKE_{tot}}$ is considerable in the whole troposphere. In particular, between the PBL top and the tropopause. Contrary, the impact of both schemes on $\mathrm{TKE_{sbg}}$ is small.

Additionally, we analyzed KES and found marginal impact of the GWD scheme, while the contribution of 3MT was larger. However, the later did not significantly change the slope of KES nor increased the noise in the pressure departure field (not shown). Based on the above analysis, switching off the GWD scheme is estimated as safe. On the other hand, the question of 3MT will remain opened (at least until the horizontal diffusion is configured).

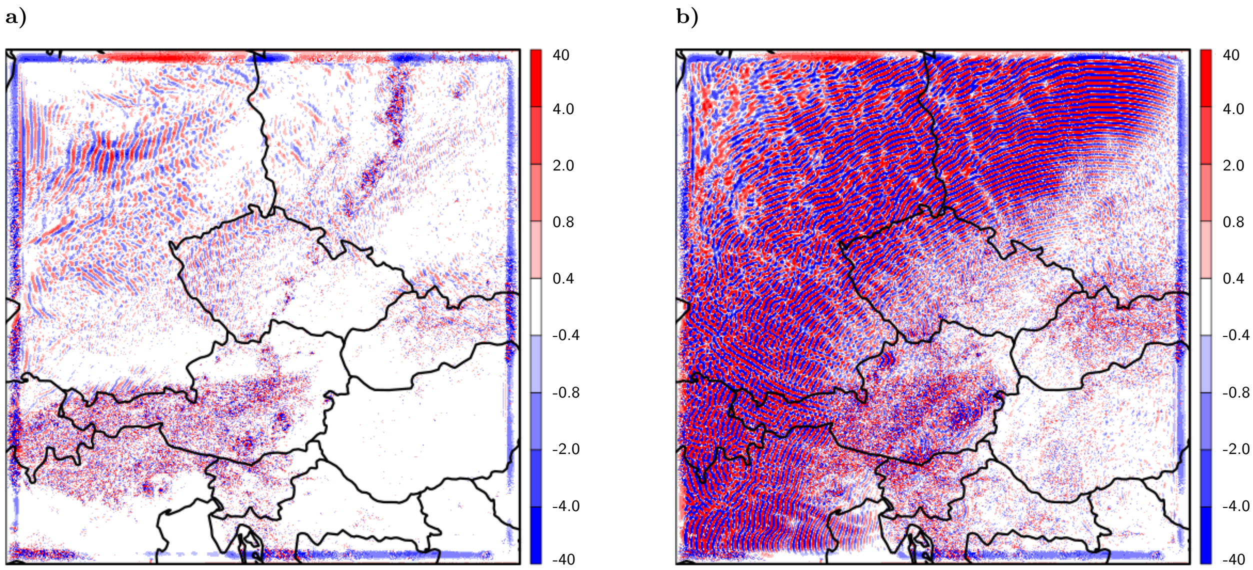

Figure 6: Pressure departure field for $\Delta x = 0.5$ km at 15 UTC 21[st] June 2018 on model level 20: **a)** reference setup with SLHD and **b)** experiment with full spectral diffusion of operational AROME-MF, i.e., without SLHD.

As an alternative to the Semi-Lagrangian Horizontal Diffusion (SLHD), used by default in the ALARO-CMC, there is a possibility to exploit the Full Spectral Diffusion (FSD) used in e.g., AROME-CMC. Aiming to find an optimal setup of the horizontal diffusion, we opted for this as our starting test. Thereby, we have utilized the operational settings of AROME-MF model. The impact on $\mathrm{TKE_{tot}}$ and related components is shown on Fig. 5a-c. Near the surface and model top, the amount of TKE_{res} and TKE_{tot} is considerably larger than for other experiments. In the middle troposphere, the impact is comparable to 3MT. Further, we analyzed KES and found decoupling with the reference near model top and significant discrepancy throughout the profile (not shown). In addition, the pressure departure fields at all levels point to significant increase of a small-scale noise. The example, for level 20, is shown of Figs. 6a-b.

Trying to optimize the FSD settings, first we increased its strength 2.5 times through related coefficients of motion variables (RDAMPDIV, RDAMPVOR and RDAMPVD). The amount of small-scale noise was reduced, while behaviour of KES and TKE_{res}/TKE_{tot} profiles improved. However, it was still far from the performance of default settings of the SLHD (not shown). Additionally, we tried to include SLHD-based diffusion on GFL fields (cloud liquid and ice, specific humidity, TKE and total turbulence energy), which further deteriorated the results (compared to reference FSD). Following this, we focused on attempts to tune the settings of the SLHD, namely its grid-point component and accompanied two spectral components, i.e., Supporting Spectral Diffusion (SSD) and Reduced Spectral Diffusion (RSD) [3, 4].

4.3 The impact of tuning the Semi-Lagrangian Horizontal Diffusion (SLHD)

The attempts to tune three-components of horizontal diffusion in ALARO-CMC utilized the experience gained from [1] and thus targeted the most sensitive parameters. However, it was proven that the sensitivity to tuning parameters decreases with increase in the horizontal resolution.

In case of the grid-point part of SLHD, we tested the most sensitive option found at $\Delta x = 1$ km (see [1] for more details). Additionally, the threshold for enhanced diffusion was decreased to SLHDD00=0.0015. However, the impact was marginal, and thus, we decided to put further attempts on hold. After that, the focus shifted towards SSD, increasing its strength 100 times (RDAMPDIVS=RDAMPVORS=RDAMPVDS=0.1). Despite the magnitude of the increase, the impact on TKE_{res} and TKE_{tot} was rather small (comparable to the impact of switching off the GWD scheme). However, the analysis of KES points to significant removal of energy from the tail of spectrum and transport towards largest scales (not shown). The impact is somewhat stronger in the stratosphere and seen as added noise to pressure departure field (Fig. 7a-b). The potential for improvement of horizontal diffusion coming from SSD is, thus, estimated as very limited, and focus shifted towards RSD.

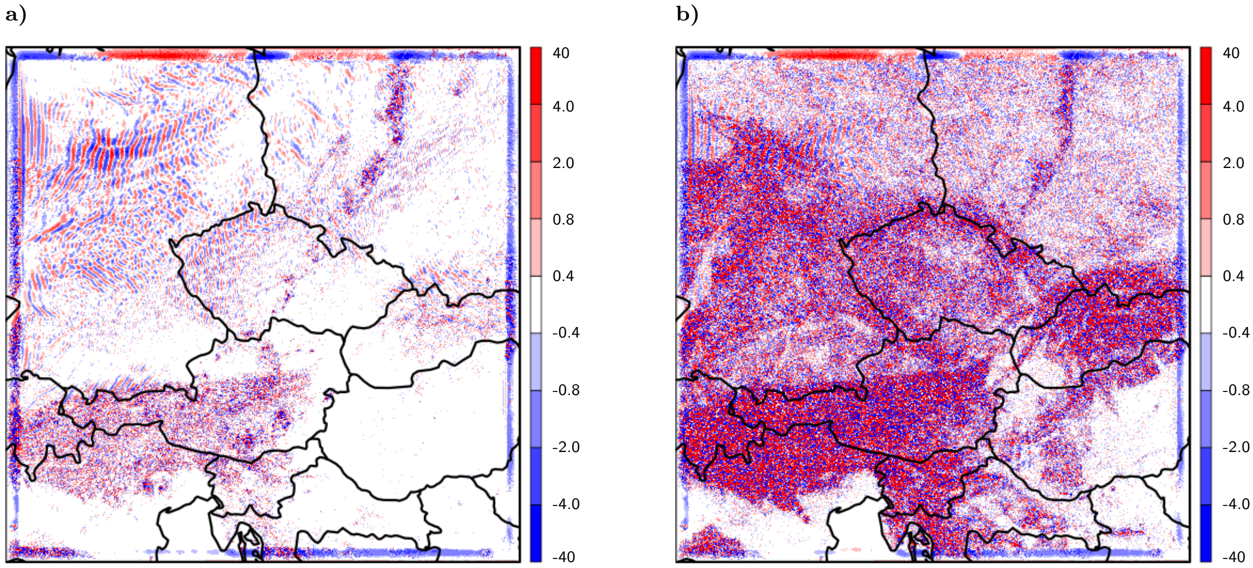

Figure 7: Pressure departure field for $\Delta x = 0.5$ km at 15 UTC 21st June 2018 on model level 20: **a)** reference setup (as on Fig. 6a) and **b)** experiment with enhanced Supporting Spectral Diffusion (SSD).

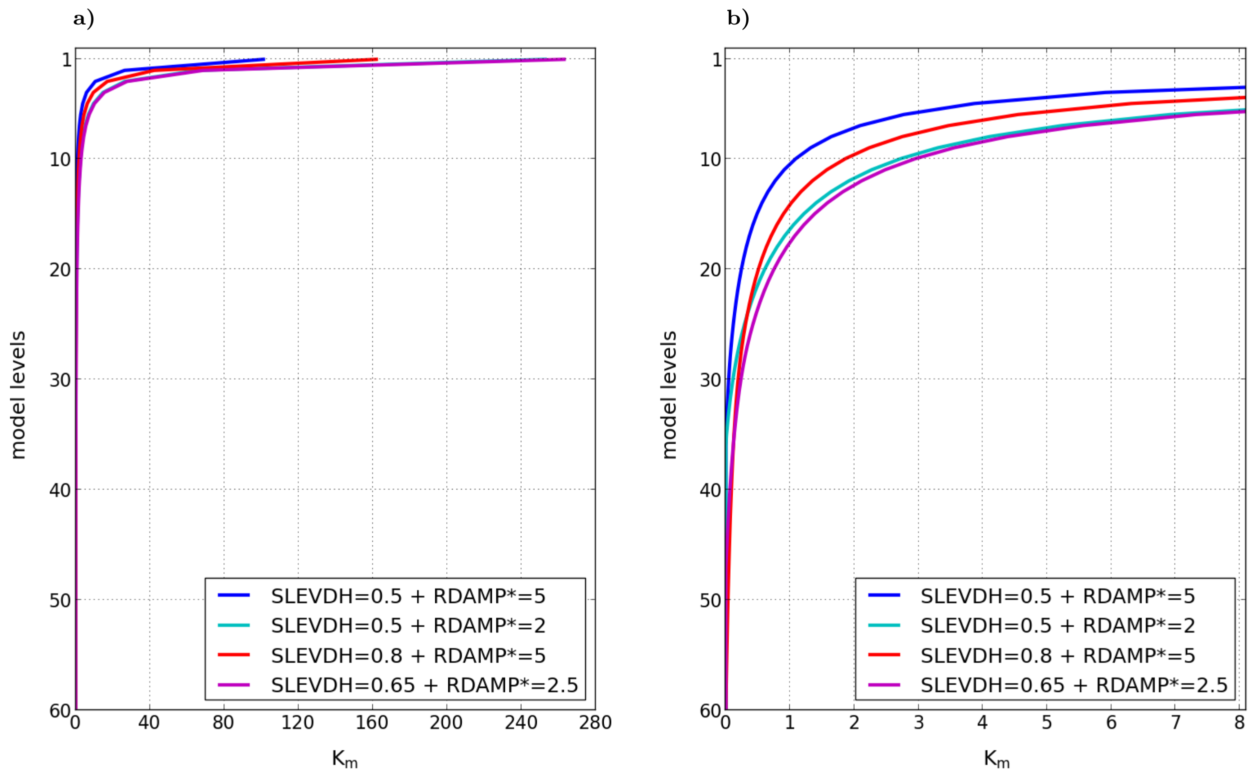

Figure 8: The profile of Resolved Spectral Diffusion (RSD) coefficient (K_m) depending on: **a)** strength parameter (RDAMP*) and profile parameter (SLEVDH) and **b)** the same as **a)** but zoomed. The * along RDAMP stands for different motion variables, i.e., divergence, vorticity and vertical divergence.

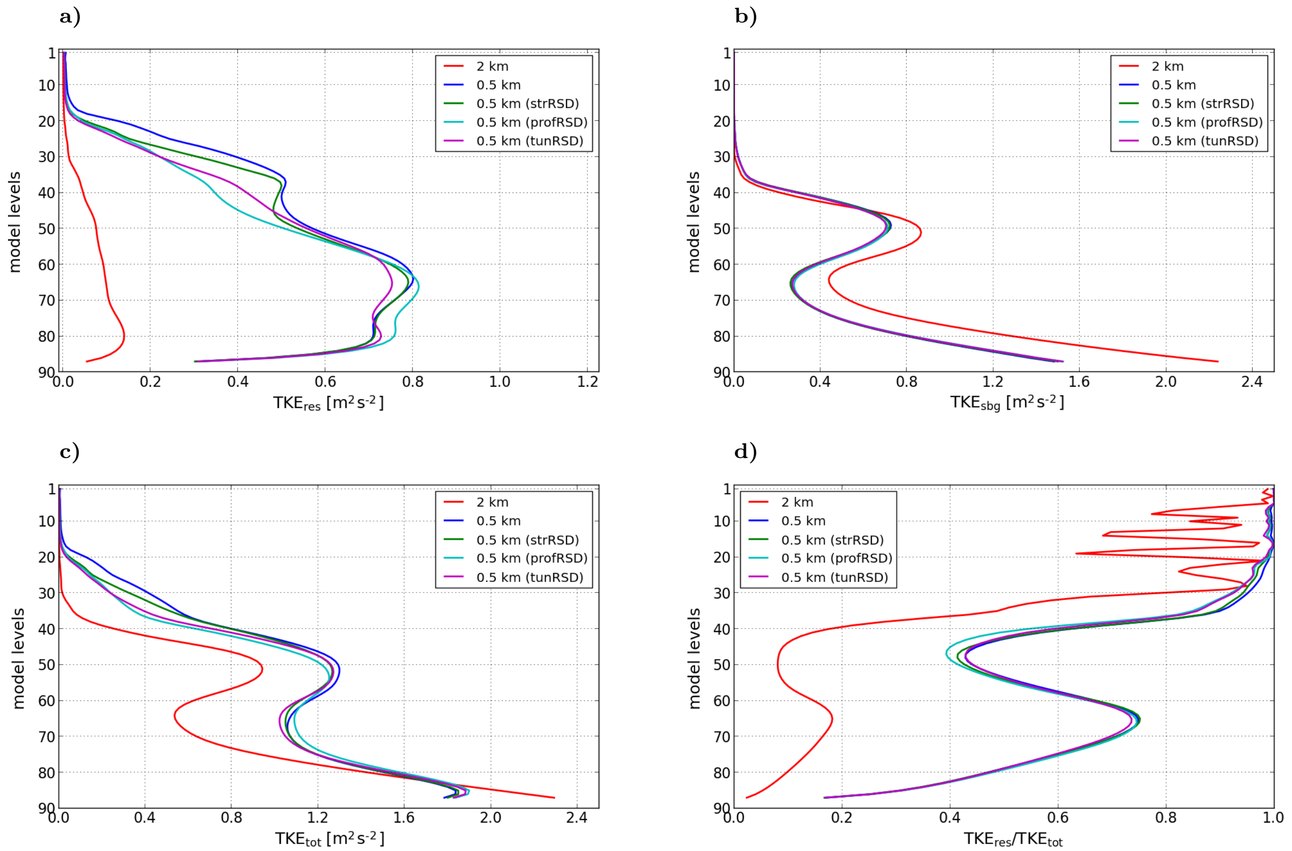

Figure 9: Spatially (over sub-domain on Fig. 1b) and temporally (between 14th and 16th hour) averaged: **a)** resolved Turbulence Kinetic Energy (TKE), **b)** subgrid TKE, **c)** total TKE and **d)** share of resolved TKE for the forecast initialized at 00 UTC 21st June 2018. References at Δx=2 [km] (red) and Δx=500 [m] (blue) correspond to Fig. 2., strRSD and profRSD are launched with stronger Reduced Spectral Diffusion (RSD; green) or applied lower in the atmosphere (cyan), while in tunRSD the tuned setup of RSD is used (magenta).

The tuning of RSD was approached, aiming to increase its strength in general (RDAMP parameters for motion variables) and affecting the profile, i.e., the starting level where RSD will start to operate (SLEVDH parameter). First, these two were tested individually and then combined so that the lower levels are also affected (46 from the model top, compared to 35 in the reference setup). The impact of both parameters individually as well as for chosen combination is shown in Fig. 8a-b. The aim was to tune RSD so that its impact is present at lower levels and that its strength near the model top remains in reasonable limits. The influence of RSD tuning on TKE_{tot} and its components is shown on Fig. 9a-c. It can be seen that the impact of SLEVDH tuning (profRSD; i.e., green curve) was stronger and led to smoothing of TKE_{res} profile above the level 50, while increasing the strength (strRSD; i.e., cyan curve) only removed a small portion of energy in the same area. On the other hand, SLEVDH tuning led to transport of additional energy into PBL, which deteriorated the results. Finally, the chosen setup (tunRSD; i.e., purple curve) seems to be a reasonable compromise throughout the profile. The impact on KES is relatively small, except above level 15. There, at medium and larger scales, the curves for tuned setup better match with those from Δx=2 [km] and Δx=1 [km] experiments. At shorter scales, the amount of energy is reduced compared to untuned counterpart (Fig. 10a-b).

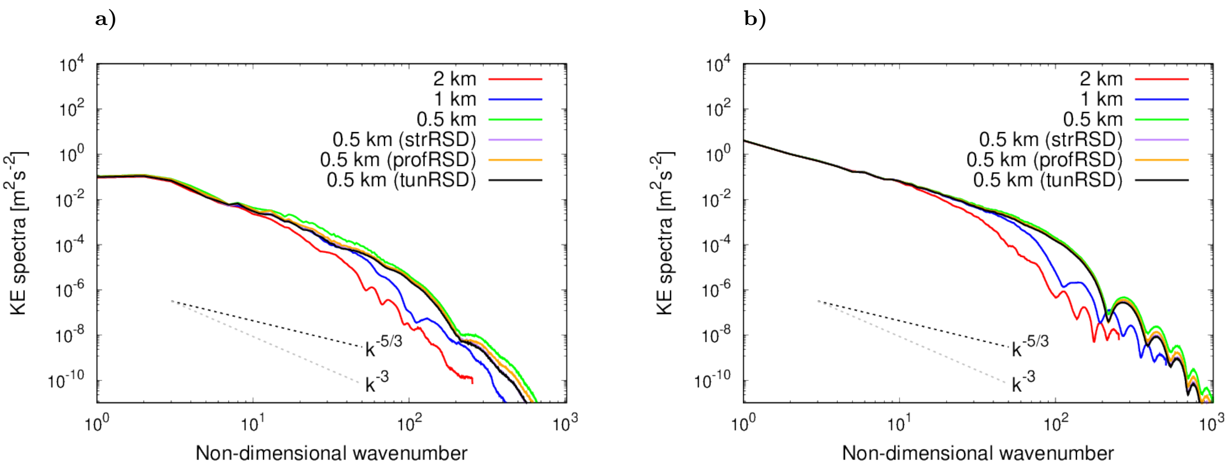

Figure 10: Kinetic energy spectra (KES) at 15 UTC 21st June 2018 for different experiments on: **a)** level 5 and **b)** level 12 (cf. caption of Fig. 9 for explanation of the legend).

The impact of tuning the grid-point part of SLHD and two accompanied spectral components is relatively small, and it led to an improvement of the model performance only between tropopause and model top. However, the deficiencies observed within the PBL and middle troposphere, i.e., accumulation of kinetic energy near the tail of spectrum, small-scale numerical noise and lack of TKE_{tot} conservation across resolutions, still exist. Due to significant reduction of TKE_{sbg} between Δx=1 km and Δx=0.5km within the PBL (compared to the change between Δx=2 km and Δx=1 km), we shall now focus on the subgrid turbulence scheme. The aim is to explore the impact of tuning the 1D scheme and missing 3D effects.

4.4 The impact of turbulent diffusion settings

Finally, we tested a sensitivity to various turbulence diffusion settings. Given that at Δx=0.5km, a significant decrease in TKE_{sbg} is observed, an attempt is made to increase it by tuning the mixing length. The related profiles of TKE_{res}, TKE_{sbg}, TKE_{tot} and share of TKE_{res} are shown in Fig. 11a-d. The tuning of vertical mixing length computation resulted in strengthening of

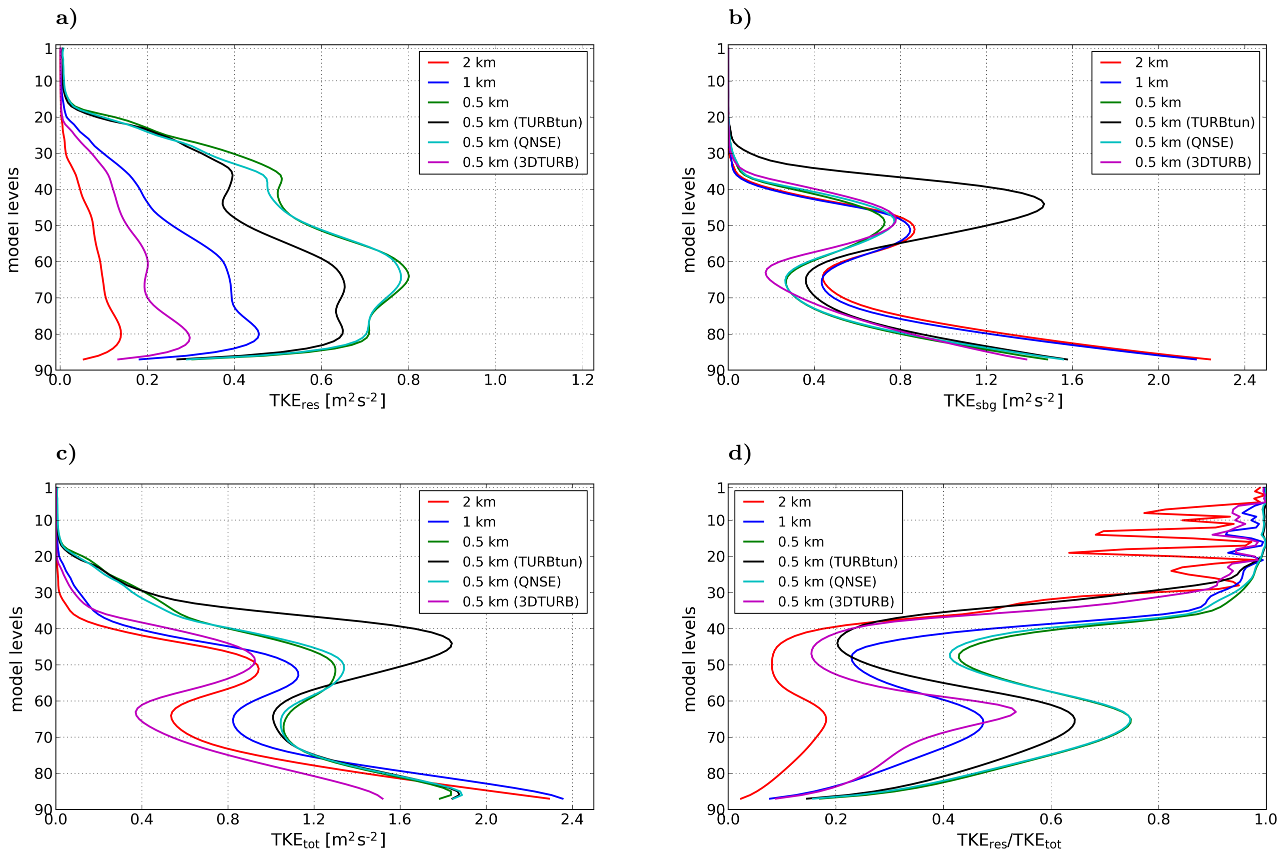

Figure 11: Spatially (over sub-domain on Fig. 1b) and temporally (between 14th and 16th hour) averaged: **a)** resolved Turbulence Kinetic Energy (TKE), **b)** subgrid TKE, **c)** total TKE and **d)** share of resolved TKE for the forecast initialized at 00 UTC 21st June 2018. References at Δx=2 [km] (red), Δx=1 [km] (blue) and Δx=500 [m] (green) correspond to Fig. 2., TURBtun and QNSE are launched with tuned vertical mixing length computatioon (black) and QNSE scheme instead of the standard TOUCANS MD2 (cyan), while the 1D+2D turbulence scheme, based on QNSE, is applied in 3DTURB (magenta).

secondary TKE_{sbg} peak near the PBL top and only minor increase within the surface layer. Following this, we wanted to investigate the impact of 3D turbulence effects. The 1D+2D scheme (available in TOUCANS) is based on QNSE closure ([5, 6, 7], which differs in values of four closure constants and stability functions from the standard MD2). We started with testing its impact within 1D turbulence scheme. As can be seen, the impact of QNSE is rather small for both TKE_{tot} and its components (Fig. 11a-d). Finally, 1D+2D closure is tested, and significant impact found for both TKE_{sbg} and TKE_{res}. The amount of TKE_{res} in 1D+2D experiment is even smaller than at Δx=1 km and very close to the profile at Δx=2 km. Overall, the horizontal diffusion with additional component seems too strong above the surface layer (Fig. 11c). However, the impact on surface layer itself is rather weak. The latter invokes inspecting the orographic roughness settings, which is the same across resolutions.

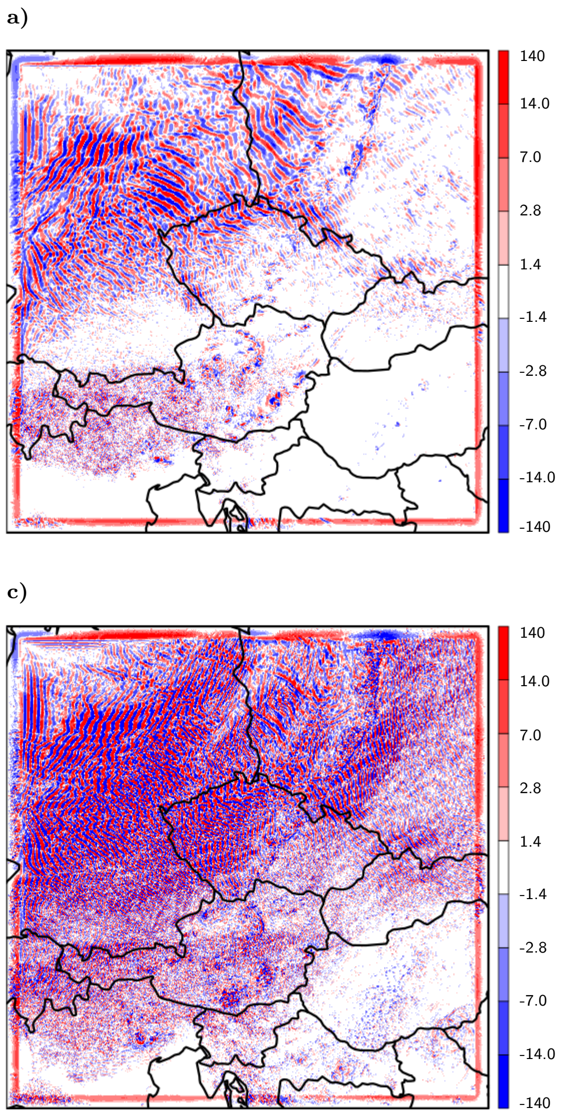

Figure 12: Pressure departure field at 15 UTC 21st June 2018 on model level 60 for: **a)** reference setup at Δx = 2 km, **b)** reference setup at Δx = 0.5 km, **c)** QNSE closure at Δx = 0.5 km and **d)** 1D+2D turbulence scheme based on QNSE at Δx = 0.5 km.

Similar to previous sets of tests, we also performed additional diagnostics. The pressure departure field at level 60 and for different experiments is shown in Fig. 12a-d. Unlike QNSE, the 1D+2D scheme removes considerable amount of small-scale features and resembles the field at Δx=2 km (Fig. 12d). However, it also contains additional elements, resulting from an increase in the horizontal resolution. As expected, KES analysis points to a significant removal of energy near the tail of spectrum and closer to the surface (Fig. 13a-b).

a) b)

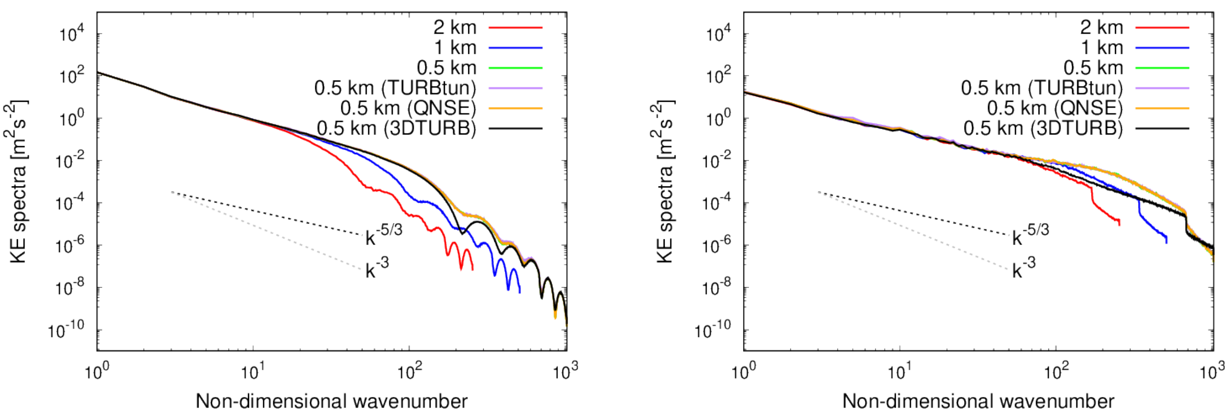

Figure 13: Kinetic energy spectra (KES) at 15 UTC 21st June 2018 for different experiments on: **a)** level 20 and **b)** level 80 (cf. caption of Fig. 11 for explanation of the legend).

The impact of 3D turbulence closure clearly drives in the positive direction. However, it still remains to optimize its interaction with the grid-point part of SLHD and two other spectral diffusion components. Additionally, a comparison with quasi-3D scheme, based on Goger's approach [8], should be conducted.

5 Conclusion and further work

During this research stay, the work on improving the performance of sub-kilometer ALARO Canonical Model Configuration (CMC) was continued. First, the behaviour of total turbulence kinetic energy (TKE_{tot}) and partitioning between its components, i.e., resolved turbulence kinetic energy (TKE_{res}) and subgrid turbulence kinetic energy, across resolutions was investigated. Further steps included inspecting the role of deep convection (3MT) and gravity wave drag (GWD) schemes (at Δx=0.5km), which were kept initially (for consistency reasons). It was found that the role of the GWD scheme is minor, while switching 3MT deteriorated the profile of TKE_{res} and TKE_{tot}. For the time being, the scheme is switched on while its setup shall be adressed later.

Following this, we opened the question of horizontal diffusion settings. The full spectral diffusion, used in AROME CMC, proved to be less efficient than default settings of Semi-Lagrangian Horizontal Diffusion (SLHD) even after several attempts of its tuning. On the other hand, the grid-point part of SLHD proved hardly tunable at (sub)-kilometer resolution. The only improvement of SLHD came from reduced spectral diffusion but limited to the layer between tropopause and model top. Finally, we investigated turbulent diffusion settings and obtained improvement with inclusion of 1D+2D option. However, further investigation and tuning is needed.

Based on the results obtained, we decided to focus further attempts on 1D+2D turbulence option and inspecting its interaction with the grid-point component of SLHD. Further, the role of horizontal components of turbulence scheme TOUCANS should be addressed, e.g., the horizontal turbulence length scale. In that context, the option based on Goger, implemented within the code during a previous stay [2], will be tested. This also includes setting its upper-limit depending on the grid-box size and following the solution of [8, 9].

Acknowledgment: The author wishes to thank to Petra Smoliková for her support and cooperation, as well as to entire ONPP department for their warm welcome and hospitality. This stay is funded by the RC-LACE project.

References

[1] M. Hrastinski. Testing the performance of Semi-Lagrangian Horizontal Diffusion (SLHD) at different horizontal resolutions. RC-LACE stay report, CHMI, Prague, Czech Republic, 2019.

[2] M. Hrastinski. Implementation of the quasi-3D turbulence scheme within the ALARO Canonical Model Configuration. RC-LACE stay report, CHMI, Prague, Czech Republic, 2022.

[3] F. Váňa. Semi-Lagrangian Horizontal Diffusion in ALADIN/ARPEGE. *RC-LACE report*, pages 1–13, 2006.

[4] F. Váňa, P. Bénard, J.-F. Geleyn, A. Simon, and Y. Seity. Semi-Lagrangian advection scheme with controlled damping: An alternative to nonlinear horizontal diffusion in a numerical weather prediction model. *Q. J. R. Meteorol. Soc.*, 134:523–537, 2008.

[5] S. Sukoriansky, B. Galperin, and V. Perov. Application of a new spectral theory of stably stratified turbulence to atmospheric boundary layers over sea ice. *Bound.-Lay. Meteorol.*, 117:231–257, 2005.

[6] S. Sukoriansky, B. Galperin, and I. Staroselsky. A quasi-normal scale elimination model of turbulent flows with stable stratification. *Phys. Fluids*, 17:085107–1–28, 2005.

[7] S. Sukoriansky, B. Galperin, and V. Perov. A quasi-normal scale elimination model of turbulence and its application to stably stratified flows. *Nonlinear Processes Geophys.*, 13:9–22, 2006.

[8] B. Goger, M. W. Rotach, A. Gohm, O. Fuhrer, I. Stiperski, and A. A. M. Holtslag. The impact of three-dimensional effects on the simulation of turbulence kinetic energy in a major alpine valley. *Bound.-Layer Meteor.*, (168):1–27, 2018.

[9] J. Smagorinski. General circulation experiments within the primitive equations. *Mon. Wea. Rev.*, (91):99–164, 1963.